Maximizing Energy Efficiency in the Vector Precoded MU-MISO Downlink by Selective Perturbation

Christos Masouros, *Senior Member, IEEE*, Mathini Sellathurai, *Senior Member, IEEE*, and Tharmalingam Ratnarajah, *Senior Member, IEEE*

***Abstract*—We propose an energy-efficient vector perturbation (VP) technique for the downlink of multiuser multiple-input–single-output (MU-MISO) systems. In contrast to conventional VP where the search for perturbation vectors involves all users' symbols, here, the perturbation is applied to a subset of the transmitted symbols. This, therefore, introduces a performance–complexity tradeoff, where the complexity is greatly reduced compared to VP by limiting the dimensions of the sphere search, at the expense of a performance penalty compared to VP. By changing the size of the subset of perturbed users, the aforementioned tradeoff can be controlled to maximize energy efficiency. We further propose three distinct criteria for selecting which users' symbols to perturb, each of which yields a different performance–complexity tradeoff. The presented analytical and simulation results show that partially perturbing the data provides a favorable tradeoff, particularly at low-power transmission where the power consumption associated with the signal processing becomes dominant. In fact, it is shown that diversity close to the one for conventional VP can be achieved at energy efficiency levels improved by up to 300% compared to VP.**

***Index Terms*—Vector perturbation, energy efficiency, complexity reduction, multi-user MIMO, non-linear precoding.**

I. Introduction

THE need to produce power- and cost-efficient mobile devises has recently stimulated interest towards precoding schemes for the multiple input multiple output (MIMO) downlink transmission. Simple forms of precoding schemes already appear in communication standards such as the 3 GPP Long Term Evolution (LTE) [1] and are expected to dominate future implementations of telecommunications networks. Capacity achieving non-linear dirty paper coding (DPC) techniques [2], [3] have been proposed for pre-subtracting interference prior to transmission. The DPC methods developed so far are in general complex as they require sophisticated sphere-search algorithms [4] to be employed at the transmitter and assume codewords with infinite length for the encoding of the data. Their suboptimal counterparts [5]–[7] offer a complexity reduction at a comparable performance. Still however, the associated complexity is prohibitive for their deployment in current communication standards.

On the other hand, linear precoding schemes based on channel inversion [8]–[14] offer the least complexity, but their performance is far from achieving the optimum maximum likelihood bound. Their non-linear adaptation, namely vector perturbation (VP) precoding [15] provides a performance improvement by introducing perturbation vectors at the transmitter to better align the data symbols to the eigenvalues of the inverse channel matrix on an instantaneous basis. This results in much improved transmit scaling factors and enhanced receive signal to noise ratios (SNRs) compared to linear precoding. The improved performance comes at the expense of an increased complexity since the search for the optimal perturbation vectors is an NP-hard problem. This is typically solved by sphere search algorithms at the transmitter with complexity that grows exponentially with the number of transmit symbols.

In response to this, the complexity of various sphere search techniques has been studied in [16]–[19] (among others) in terms of search nodes visited and search lattice volumes. A number of techniques have been proposed towards reducing the complexity of VP precoding (e.g. [20]–[27]). All the above designs achieve the complexity reduction at the expense of an inferior performance compared to conventional VP. In [23] a search over a reduced lattice is proposed, based on empirical observations of the relation between the instantaneous symbols and the optimum perturbation vectors. Further work in [24] has proposed the decoupling of the perturbation optimization in the real and imaginary domain of the data symbols thus offering a lower complexity compared to the joint optimization approach. Finally, in [28] a joint linear and non-linear precoding scheme is proposed for the next generation of cellular systems where the legacy users employ existing linear precoding techniques from the communication standards, while the new added users in the network employ VP precoding.

Inspired by this joint linear/non-linear approach, in this paper we explore a partial perturbation technique where from the total number of information symbols to transmit, the perturbation quantities are applied only to a subset of these symbols. The

Manuscript received July 31, 2013; revised December 2, 2013, March 17, 2014, and May 21, 2014; accepted June 3, 2014. Date of publication June 6, 2014; date of current version September 8, 2014. This work was supported by the Royal Academy of Engineering, U.K., by the Seventh Framework Program for Research of the European Commission under Grant HARP-318489, and by the EPSRC under Grant EP/I037156/1. The associate editor coordinating the review of this paper and approving it for publication was S. C. Liew.

C. Masouros is with the Department of Electronic and Electrical Engineering, University College London, London WC1E 7JE, U.K. (e-mail: chris.masouros@ieee.org).

M. Sellathurai is with the School of Engineering and Physical Sciences, Heriot-Watt University, Edinburgh EH14 4AS, U.K. (e-mail: mathini@ieee.org).

T. Ratnarajah is with the School of Engineering, The University of Edinburgh, Edinburgh EH9 3JL, U.K. (e-mail: t.ratnarajah@ieee.org).

Color versions of one or more of the figures in this paper are available online at http://ieeexplore.ieee.org.

Digital Object Identifier 10.1109/TWC.2014.2329480

This work is licensed under a Creative Commons Attribution 3.0 License. For more information, see http://creativecommons.org/licenses/by/3.0/

rest of the symbols are transmitted without perturbation in a fashion similar to channel inversion precoding. We see in the results that the perturbation of a subset of symbols is typically enough to align the transmit symbols with the eigenvalues of the channel, thus approaching the diversity offered by the full VP as applied conventionally. At the same time, by saving significant computational complexity, the proposed scheme offers a favorable energy efficiency compared to VP. Finally, by judiciously selecting the symbols to perturb, additional performance gains are achievable, at the cost of added complexity. To optimize this tradeoff, we propose a number of associated selection schemes.

It should be noted that the proposed schemes do not constitute user selection schemes such as for example [22] where a subset of the users' symbols are selected for transmission. Indeed here all users' symbols are transmitted. The selection refers to choosing which of the transmit symbols to perturb. Moreover, compared to previous works on complexity reduction for VP [23]–[27], this work explores a distinct new approach based on partial symbol perturbation as opposed to a full perturbation. The proposed can be applied on top of other complexity reduction techniques to further reduce complexity compared to the case where the full sphere search is carried out. Since here we explore a perturbation for a subset of the transmit symbols, complexity gains will still be observed. However, to keep the focus of this work on the central idea, we only use conventional VP with a limited search lattice proposed in [23], as the reference technique.

For reasons of clarity we list the contributions of the present work:

1) We introduce a new selective VP scheme that reduces the complexity with respect to conventional VP schemes,
2) To optimize the performance-complexity tradeoff, we further propose three distinct criteria for the selection of the transmit symbols to perturb,
3) We calculate and compare analytically the complexity of conventional and proposed techniques, and prove the complexity benefits of the proposed approach mathematically, based on the volume of the search space associated with each of the techniques,
4) We quantify the performance-complexity tradeoff of conventional and proposed VP, by introducing a energy efficiency metric that combines sum rate, transmit power and complexity and prove the enhanced tradeoff for the proposed scheme. We demonstrate that this metric can be used to design an energy efficient communication link by optimizing the number of perturbed users required in the proposed VP.

The rest of the paper is organized as follows. Section II illustrates the MISO channel model used in this paper and briefly describes conventional VP precoding. In Section III the proposed selective VP is presented, along with the associated symbol selection techniques. Section IV presents a complexity analysis of the proposed techniques, based on the volume of the search space associated with the sphere encoder. Analytical sum rate expressions are given in Section V, where the energy efficiency metric to evaluate the performance-complexity tradeoff is introduced. Finally numerical results are illustrated and discussed in Section VI and conclusions are summarized in Section VII.

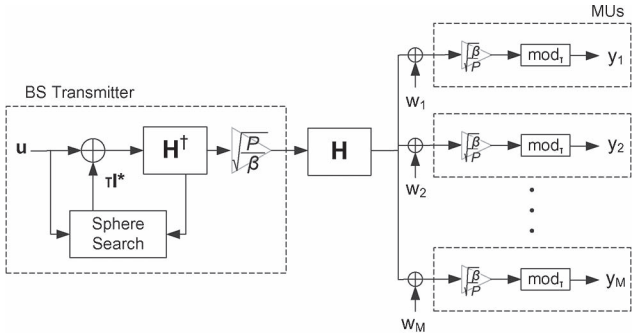

Fig. 1. Block diagram of VP in the MU-MISO downlink.

II. MU-MISO Channel Model and VP

A. MU-MISO Channel Model

We consider a downlink system comprised of a single base station (BS) equipped with N transmit antennas and $M \leq N$ users with a single receive antenna each. The received signals of all antennas can be represented by the vector

$$\mathbf{r} = \mathbf{H} \cdot \mathbf{x} + \mathbf{w} \tag{1}$$

Here $\mathbf{r} \in \mathbb{C}^{M\times 1}$ and $\mathbf{H} \in \mathbb{C}^{M\times N} \sim \mathcal{CN}(0, \mathbf{I}_M \otimes \mathbf{I}_N)$ contains the frequency flat fading channel coefficients with the (m,n)-th element $h_{m,n}$ being the complex-Gaussian channel tap between the n-th transmit and the m-th receive antenna. Also, $\mathbf{x} \in \mathbb{C}^{N\times 1}$ is the vector with the symbols transmitted by the N transmit antennas and $\mathbf{w} \in \mathbb{C}^{M\times 1} \sim \mathcal{CN}(0, \sigma^2\mathbf{I}_M)$ is the vector of the additive white Gaussian noise (AWGN) components at the M receive antennas. We note here that, to focus the paper on the proposed idea and comparisons to conventional VP, and following the modeling in the most relevant works, the above model ignores factors such as path loss that could create variations in the SNRs of different users. For such scenarios there exist solutions which constitute variants of the conventional VP in the form of block diagonalized VP [26], which the proposed scheme can apply on to further reduce complexity. For the purposes of the analysis below, full knowledge of channel state information (CSI) is assumed at the BS transmitter, which is a common assumption in the VP literature.

B. VP Precoding

VP employs a channel inversion precoding matrix and applies a perturbation on the transmitted symbols such that the useful signal power at the receiver is maximized. The block diagram is shown in Fig. 1. The transmitted signal is given by [15]

$$\mathbf{x} = \sqrt{\frac{P}{\beta}}\mathbf{F}(\mathbf{u} + \tau\mathbf{l}^{\star}) \tag{2}$$

where $\mathbf{F}$ is the precoding matrix, $\mathbf{u} \in \mathbb{C}^{M\times 1}$ is the data symbol vector,

$$\beta = \|\mathbf{F}(\mathbf{u} + \tau\mathbf{l}^{\star})\|^2 \tag{3}$$

is the transmit power scaling factor so that $E\{\|\mathbf{x}\|^2\} = P$ and $\mathbf{l}^\star \in \mathbb{C}^{M\times 1}$ is the selected perturbation vector with integer entries that will be detailed in the following. Also $\tau = 2|c|_{\max} + \Delta$, where $|c|_{\max}$ is the absolute value of the constellation symbol with the maximum magnitude and Δ denotes the minimum Euclidean distance between constellation symbols. The precoding matrix can be a channel inversion matrix in the form $\mathbf{F} = \mathbf{H}^H(\mathbf{H}\mathbf{H}^H)^{-1}$ or a regularized channel inversion matrix $\mathbf{F} = \mathbf{H}^H(\mathbf{H}\mathbf{H}^H + \alpha\mathbf{I})^{-1}$. For simplicity we focus on the former in this paper, while the benefits of the proposed ideas on the latter are intuitive. For the special case of channel inversion precoding [8] we have $\tau\mathbf{l}^\star = \mathbf{0}_M$, where $\mathbf{0}_M$ is the all zero $M \times 1$ vector. Based on the above expressions the received symbol vector can be calculated as

$$\mathbf{r} = \sqrt{\frac{P}{\beta}}(\mathbf{u} + \tau\mathbf{l}^\star) + \mathbf{w} \tag{4}$$

At the receiver the signal is first scaled back to eliminate the effect of the transmit scaling factor and then fed to a modulo operator to remove the perturbation quantity $\tau\mathbf{l}^\star$. The output of the modulo stage is given as

$$\mathbf{y} = \mathrm{mod}_\tau\left[\sqrt{\frac{\beta}{P}}\mathbf{r}\right] = \mathrm{mod}_\tau\left[\mathbf{u}+\tau\mathbf{l}^\star+\sqrt{\frac{\beta}{P}}\mathbf{w}\right] = \mathbf{u}+\mathbf{n} \tag{5}$$

where $\mathrm{mod}_\tau[x] = f_\tau(\Re(x)) + \mathrm{j}\cdot f_\tau(\Im(x))$ and

$$f_\tau(x) = x - \left\lfloor \frac{x+\tau/2}{\tau} \right\rfloor \tau \tag{6}$$

In the above, vector $\mathbf{n}$ in (5) denotes the equivalent noise vector at the receiver after the scaling and modulo operation.

C. Perturbation Vector Selection

To maximize the signal component in the received symbols or equivalently minimize the noise amplification, the perturbation vectors $\mathbf{l}^\star$ should be chosen such that β is minimized in (5). Hence we have

$$\mathbf{l}^\star = \arg\min_{\mathbf{l}\in\mathbb{Z}^M+\mathrm{j}\mathbb{Z}^M} \|\mathbf{F}(\mathbf{u}+\tau\mathbf{l})\|^2 \tag{7}$$

For complex symbol alphabets, the optimization in (7) is a $2M$-dimentional real integer lattice problem, known to be NP-hard. Sphere search techniques are typically employed to solve the minimization. A computationally efficient and flexible implementation of sphere search is the Schnorr-Euchner (SE) algorithm [29], which we adopt in this paper and modify for the purposes of the proposed VP design. We note that the decoupled optimization of the precoding matrix and the perturbation vectors separately is essential in transforming the VP optimization in a least squares problem and solving it by sphere search techniques. The joint optimization of $\mathbf{F}$ and $\mathbf{l}$ would involve a highly complex optimization for which no standard solvers exist.

III. Selective Vector Precoding (SVP)

It is well established in the literature that the volume and associated complexity of VP grows exponentially with the number of search dimensions n. To limit this complexity we explore a partial perturbation scheme where a subset of L symbols out of the M total transmitted symbols is perturbed by means of the perturbation vectors $\mathbf{l}$. Clearly this reduces the number of dimensions to L and therefore the complexity now grows with L. The associated optimization can be written as

$$\mathbf{l}^\star = \arg\min_{\mathbf{l}\in\mathbb{Z}^L+\mathrm{j}\mathbb{Z}^L} \left\|\bar{\mathbf{F}}\left(\bar{\mathbf{u}} + \tau\begin{bmatrix}\mathbf{0}_{M-L}\\ \mathbf{l}_L\end{bmatrix}\right)\right\|^2 \tag{8}$$

Here $\bar{\mathbf{u}}$ and $\bar{\mathbf{F}}$ denote the appropriate re-ordering of the data vector and the columns of matrix $\mathbf{F}$ to allow for the selection of the symbols to be perturbed, as detailed in the following. By partitioning the precoding matrix as $\bar{\mathbf{F}} = [\bar{\mathbf{F}}_{M-L}\ \bar{\mathbf{F}}_L]$ where $\bar{\mathbf{F}}_{M-L} \in \mathbb{C}^{M\times(M-L)}$ and $\bar{\mathbf{F}}_L \in \mathbb{C}^{M\times L}$, (8) can be transformed into

$$\mathbf{l}^\star = \arg\min_{\mathbf{l}\in\mathbb{Z}^L+\mathrm{j}\mathbb{Z}^L} \|\bar{\mathbf{F}}\bar{\mathbf{u}} + \tau\bar{\mathbf{F}}_L\mathbf{l}_L\|^2 \tag{9}$$

Clearly (9) is L-dimensional and can be solved by standard sphere search techniques. The receive processing required for SVP is identical to the one for conventional VP in Fig. 1.

Further expanding (9) we have

$$\mathbf{l}^\star = \arg\min_{\mathbf{l}\in\mathbb{Z}^L+\mathrm{j}\mathbb{Z}^L} \left\{\|\mathbf{F}\mathbf{u}\|^2 + \tau^2\|\bar{\mathbf{F}}_L\mathbf{l}_L\|^2 + 2\tau\Re(\bar{\mathbf{u}}^H\bar{\mathbf{F}}^H\bar{\mathbf{F}}_L\mathbf{l}_L)\right\} \tag{10}$$

or equivalently

$$\mathbf{l}^\star = \arg\min_{\mathbf{l}\in\mathbb{Z}^L+\mathrm{j}\mathbb{Z}^L} \left\{\tau^2\|\bar{\mathbf{F}}_L\mathbf{l}_L\|^2 + 2\tau\Re(\bar{\mathbf{u}}^H\bar{\mathbf{F}}^H\bar{\mathbf{F}}_L\mathbf{l}_L)\right\}. \tag{11}$$

We note that $\tau^2\|\bar{\mathbf{F}}_L\mathbf{l}_L\|^2 \le \tau^2 tr(\bar{\mathbf{F}}_L^H\bar{\mathbf{F}}_L)\|\mathbf{l}_L\|^2$, where $tr(.)$ denotes the trace of a matrix, though this is not a tight bound. It can be observed that the selection of symbols to perturb by means of the vectors $\mathbf{l}_L$ becomes a selection between the most appropriate columns of the precoding matrix to form $\bar{\mathbf{F}}_L$.

We next introduce the proposed selection techniques, along with the associated algorithms in the following tables. We use [] to denote an empty matrix, $\{\mathbf{X}\}_y$ to denote the y columns of $\mathbf{X}$, $\mathtt{sort}(\mathbf{x})$ to represent the ordering of the elements in vector $\mathbf{x}$ in an ascending manner, $\mathtt{nchoosek}(\mathtt{n},\mathtt{k})$ to denote all the possible combinations of groups with size k and n candidates and $\mathtt{SE}\{k,\mathbf{x},\mathbf{A}\}$ to denote the Schnorr-Euchner algorithm [29] that minimizes the integer least squares problem $\arg\min_{\mathbf{y}} \|\mathbf{x} - \mathbf{A}\mathbf{y}\|$ with dimension size k.

A. Random Selection (SVP-RS)

The simplest selection scheme applies random user selection, and involves a random re-ordering of the columns of $\mathbf{F}$. The implementation algorithm is shown in Table III.A. Without loss of generality, for a large number of channel instantiations, this can be equivalently implemented by simply choosing the last L columns of the precoding matrix. The partial perturbation of the symbols on its own greatly reduces the computational complexity and also outperforms channel inversion. By increasing the

TABLE III.A

ALGORITHM SVP-RS

$\mathbf{F} = [\mathbf{F}_{M-L}, \mathbf{F}_L]$

$\mathbf{l}^\star = \mathtt{SE}\{L, \mathbf{Fu}, -\mathbf{F}_L\tau\}$

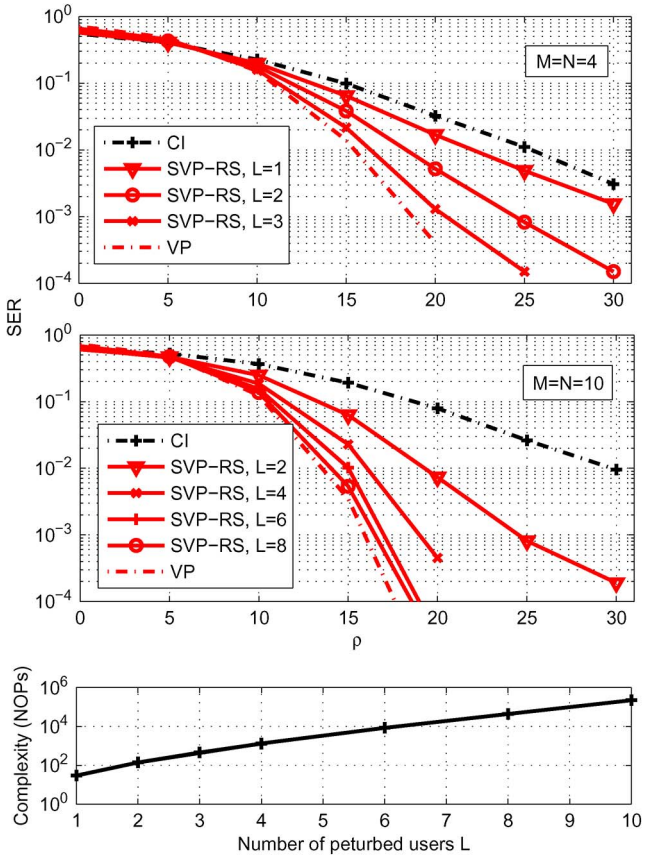

Fig. 2. Error rates and Complexity of SVP-RS with L for $N = M = 4$ and $N = M = 10$, 4-QAM.

number of perturbed symbols L, SVP-RS quickly approaches the diversity order of conventional VP.

This is shown in the preliminary results in Fig. 2 where the symbol error rate performance and complexity in terms of numbers of floating point operations (NOP) of SVP-RS is shown for increasing numbers of perturbed users L, for the cases of $N = M = 4$ and $N = M = 10$ respectively. A system employing 4-QAM modulation is assumed and perfect channel state information (CSI) is available at the transmitter. We note that the performance for VP in general is governed by the scaling factor β [15] which is unique and common for all MUs. Therefore the average performance shown here applies to all users in the system. It can be seen that the performance of SVP-RS improves from that of CI $(L = 0)$ to VP $(L = N)$ as the number of perturbed users increases. In the case for $N = M = 10$ the performance of SVP converges faster to that of VP as the number of perturbed users increases. In addition, the complexity benefits are more significant as near-VP performance is achieved for moderate values of L. For example the complexity is more than 5000 times more for VP compared to SVP with $L = 2$ with a respective SNR gain of 7 dB. It can therefore be observed that SVP becomes more useful for systems with larger numbers of users as the tradeoff between the performance loss and gains in complexity becomes more favorable. As SVP-RS is the simplest of the selection schemes and is equivalent to SVP without selection, we shall use it as reference hereof.

TABLE III.B

ALGORITHM SVP-OS

$\mathbf{b} = \mathtt{nchoosek}(M, L)$

$\mathtt{for}\ i = 1\ \mathtt{to}\ \binom{M}{L}\ \mathtt{do}$

$\quad \bar{\mathbf{F}}_L^i := \{\mathbf{F}\}_{\mathbf{b}(i)}$

$\quad \mathbf{l}^i = \mathtt{SE}\{L, \mathbf{Fu}, -\bar{\mathbf{F}}_L^i\tau\}$

$\quad \aleph_i = ||\mathbf{Fu} + \tau\bar{\mathbf{F}}_L^i\mathbf{l}^i||$

$\mathtt{end}$

$\mathbf{l}^\star = \mathbf{l}^{\arg\min_i\{\aleph_i\}}$

B. Optimal Selection (SVP-OS)

The optimal symbol selection involves the calculating of the signal norm

$$\aleph_i = \left\|\mathbf{Fu} + \tau\bar{\mathbf{F}}_L^i\mathbf{l}_L\right\|, \quad i \in 1, \ldots \binom{M}{L} \tag{12}$$

for all possible groups of transmit symbols with size L and selecting the group of transmit symbols that jointly minimizes the signal norm as

$$\bar{\mathbf{F}}_L = \arg\min_i \left\|\mathbf{Fu} + \tau\bar{\mathbf{F}}_L^i\mathbf{l}_L\right\|, \quad i \in 1, \ldots \binom{M}{L} \tag{13}$$

The implementation algorithm is shown in Table III.B. Clearly, this provides the best possible performance for SVP for a given number of perturbed users L, but also involves the highest computational complexity as an L-dimensional sphere search must be carried out for each of the $\binom{M}{L} = M!/(M-L)!L!$ candidate symbol groups, where (.)! denotes the factorial operation. It will be shown however that SVP-OS provides a close-to-VP diversity for low numbers of L.

C. Decoupled Selection (SVP-DS)

For a lower-complexity alternative with respect to SVP-OS we explore a decoupled approach where the symbols selected are those that provide the most improvement in the transmit signal norm when VP is applied on these symbols individually. The implementation algorithm is shown in Table III.C. We therefore apply VP to a single symbol at a time to obtain the metric

$$\aleph_k = \|\mathbf{Fu} + \tau\mathbf{f}_k l_k\|, \quad k \in 1, \ldots M \tag{14}$$

with $\mathbf{f}_k$ denoting the k-th column vector of $\mathbf{F}$. We subsequently select the group of L users with the symbols that provided the L lowest signal norms $\aleph_k$

$$\bar{\mathbf{F}}_L = \{\acute{\mathbf{F}}\}_{1:L} \tag{15}$$

where $\{\mathbf{X}\}_{1:L}$ denotes the first L columns of matrix $\mathbf{X}$, and $\acute{\mathbf{F}}$ is the precoding matrix $\mathbf{F}$ with columns re-ordered according to increasing $\aleph_i$. The perturbation vectors are then obtained by a final L-dimensional search between the selected users.

TABLE III.C

ALGORITHM SVP-DS

for $i = 1$ to M do
  $\mathbf{f}_i := \{\mathbf{F}\}_i$
  $l^i = \mathrm{SE}\{1, \mathbf{Fu}, -\mathbf{f}_i\tau\}$
  $\aleph_i = ||\mathbf{Fu} + \tau\mathbf{f}_i l^i||$
end
$[m, n] = \mathrm{sort}(\aleph_i)$
$\mathbf{l}^\star = \mathbf{l}^{\{n\}_{1:L}}$

TABLE III.D

ALGORITHM SVP-SS

$\bar{\mathbf{F}}_L = [\,]$
$\mathbf{\Phi} = \mathbf{F}$
for $k = 1$ to L do
  for $i = 1$ to $M - k + 1$ do
    $\mathbf{f}_i := \{\mathbf{\Phi}\}_i$
    $\bar{\mathbf{F}}_L^i := [\bar{\mathbf{F}}_L, \mathbf{f}_i]$
    $\mathbf{l}_k^i = \mathrm{SE}\{k, \mathbf{Fu}, -\bar{\mathbf{F}}_L^i\tau\}$
    $\aleph_k^i = ||\mathbf{Fu} + \tau\bar{\mathbf{F}}_L^i\mathbf{l}_k^i||$
  end
  $m = \arg\min_i\{\aleph_k^i\}$
  $\bar{\mathbf{F}}_L := [\bar{\mathbf{F}}_L, \mathbf{f}_m]$
  $\mathbf{\Phi} := \{\mathbf{\Phi}\}_{1:i-m, m+1:M-k+1}$
  $\mathbf{l}_k^\star = \mathbf{l}_k^m$
end
$\mathbf{l}_L^\star = \mathbf{l}_k^\star$

D. Sequential Selection (SVP-SS)

As a final alternative with intermediate performance and complexity between SVP-OS and SVP-DS we propose to sequentially select users according to the minimum norm criterion. The implementation algorithm is shown in Table III.D. We start with the column of $\mathbf{F}$ corresponding to the symbol that yields the minimum norm after perturbation. We then add columns to $\bar{\mathbf{F}}_L$ by selecting the additional symbol that minimizes the signal norm after joint perturbation with the previously selected symbols. That is, starting with an empty matrix $\bar{\mathbf{F}}_L$, we initially choose the first column according to

$$\arg\min_{k_1} \|\mathbf{Fu} + \tau\mathbf{f}_{k_1} l_{k_1}\|, \quad k_1 \in 1, \ldots M \tag{16}$$

and subsequently add the n-th user by stacking the appropriate column of $\mathbf{F}$ to form the $M \times n$ matrix $\bar{\mathbf{F}}_{k_n} = [\bar{\mathbf{F}}_{k_{n-1}}, \mathbf{f}_{k_n}]$ according to

$$\bar{\mathbf{F}}_{k_n} = \arg\min_{k} \left\|\mathbf{Fu} + \tau\bar{\mathbf{F}}_{k_n}\mathbf{l}_{k_n}\right\|, \quad k_n \in 1, \ldots M, \quad k_n \neq k_1, k_2, \ldots, k_{n-1} \tag{17}$$

In the above $[\mathbf{X}, \mathbf{Y}]$ denotes the horizontal stacking of matrices $\mathbf{X}, \mathbf{Y}$.

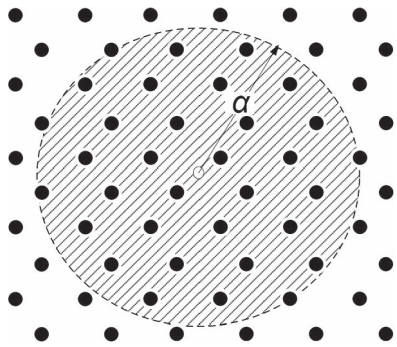

Fig. 3. Geometrical representation of the 2-dimensional integer-lattice sphere search problem.

IV. Computational Complexity

To evaluate the performance-complexity tradeoff and overall energy efficiency of the proposed schemes, in this section we study the computational complexity of selective VP. We start by introducing an upper bound of the volume searched by the sphere encoder for the L-dimensional lattice and use this to calculate the average number of nodes visited by the encoder. Finally, using an average value for the number of numerical operations (NOPs) per node, we derive the average NOPs carried out by the sphere encoder, for each of the symbol selection techniques.

A. Search Volume

It has been observed in [18] and references therein that the complexity of the SE search is proportional to the volume of the region being searched in the lattice space. At the k-th search layer this volume is a hypersphere with maximum radius α_k. A geometrical illustration of this is shown in Fig. 3 for a 2-dimensional lattice. Here the dots represent the lattice points and the area inside the circle denotes the area of candidate points searched, based on the search radius α. For the proposed SVP the search space is L-dimensional, as opposed to the M-dimensional space for the full VP search. In the following, we use these key observations to attain a complexity evaluation for SVP, following the methodology of [17], [18].

Theorem 1: Define the search volume for the k-th search layer with radius α_k as $\mathcal{V}_k(\alpha_k)$. For the complexity C associated with SVP in a L-dimensional lattice we have

$$C \propto \mathcal{V}_L(\infty) \tag{18}$$

for which

$$\mathcal{V}_L(\infty) \leq \frac{\pi^{\frac{L}{2}}}{2^L\Gamma(L/2+1)}\phi_L^L \tag{19}$$

where $\phi_k = \sqrt{r_{1,1}^2 + r_{2,2}^2 + \ldots + r_{k,k}^2}$, $k = 1, \ldots, L$, $r_{i,i}$ are the diagonal elements of matrix $\mathbf{R}$ obtained from the QR decomposition

$$[\mathbf{Q}, \mathbf{R}] = QR(-\bar{\mathbf{F}}_L\tau) \tag{20}$$

and $\Gamma(.)$ denotes the gamma function.

Proof: The proof of Theorem 1 closely follows the sphere search volume analysis in [18]. It can be seen that the Schnorr-Euchner search starts with an infinite search radius at the highest search layer for $k = L$ which is decreased at each layer according to the minimum observed weight in the previous layer. Hence, the aforementioned radius a_k is adaptive on a layer-by-layer basis. Accordingly, it has been shown in [18], [20] that the volume of the search space for the k-th layer follows

$$\mathcal{V}_k(\alpha_k) \leq \frac{\pi^{\frac{k}{2}}}{\Gamma(k/2+1)} \prod_{n=1}^{k} \alpha_n \leq \frac{\pi^{\frac{k}{2}}}{\Gamma(k/2+1)} \alpha_k^k \qquad (21)$$

where the second term represents the volume of a hyper-sphere with radius α_n in the n-th dimension and the third term a hyper-sphere with radius α_k in all dimensions. The second inequality in (21) therefore stems from the fact that the radius decreases with increasing layers and therefore the volume of the search space is upper bounded by the volume of the hyper-sphere with the maximum radius in all dimensions. It addition it is well known from lattice theory that $\alpha_k \leq \phi_k/2$ for all k, where ϕ_k is defined as in the theorem above [18]. Therefore, using (21) we have the following upper-bound

$$\mathcal{V}_k(\infty) \leq \frac{\pi^{\frac{k}{2}}}{\Gamma(k/2+1)} \prod_{n=1}^{k} \frac{\phi_n}{2} \leq \frac{\pi^{\frac{k}{2}}}{2^k \Gamma(k/2+1)} \phi_k^k \qquad (22)$$

■

Clearly, where for conventional VP the volume of the M-layered search is given by $\mathcal{V}_M(\infty)$, for the proposed SVP the volume of the L-dimensional sphere search with $L < M$ is bounded by $\mathcal{V}_L(\infty)$. Since $\mathcal{V}_k(\infty)$ is monotonically increasing with k we have $\mathcal{V}_L(\infty) \leq \mathcal{V}_M(\infty)$ and therefore the sphere search involved in SVP has a reduced complexity compared to the one for VP.

In the above theorem, the complexity reduction with SVP has been shown by means of search space volume. A complexity comparison between VP and SVP in terms of elementary operations is shown analytically in the next section and numerically in the results section in the following.

B. Numerical Operations

The above analysis can be used to obtain an upper bound on the expected numerical operations associated with the proposed precoding. Note that, as the search volume is associated with the search tree complexity, the analysis below focuses only on the operations required for the search stage, ignoring the pre- and post-search operations such as the QR decomposition etc. This is a common practice in the literature [16]–[18].

It was shown in [17] that for an infinite lattice,[1] the expected number of lattice points contained inside a k-dimensional hypersphere of radius α is given as

$$E_p(k, \alpha^2) = \sum_{q=0}^{\infty} \varphi\left(\frac{\alpha^2}{2(\sigma^2+q)}, \frac{k}{2}\right) \cdot r_k(q) \qquad (23)$$

where

$$\varphi(x, \kappa) = \int_0^x \frac{t^{\kappa-1}}{\Gamma(\kappa)} e^{-t} dt \qquad (24)$$

is the normalized incomplete gamma function and $r_\kappa(x)$ denotes the number of ways a non-negative integer x can be represented as a sum of κ squares of integers. The closed form definition of $r_\kappa(x)$ is a classical number-theory problem, well studied in the literature [17], [20]. Clearly, based on the above we can derive upper bounds for expected numbers of nodes visited by the sphere encoder.

Using (23), for the volume in (22) of a hypersphere with radius $\phi_k/2$ in all dimensions we have the straightforward upper bound

$$\begin{aligned} p(k) &\leq E_p\left(k, \left(\frac{\phi_k}{2}\right)^2\right) \\ &= \sum_{q=0}^{\infty} \varphi\left(\frac{\frac{\phi_k^2}{4}}{2(\sigma^2+q)}, \frac{k}{2}\right) \cdot r_k(q) \triangleq \tilde{p}(k) \end{aligned} \qquad (25)$$

The complexity in numbers of numerical operations for a generic Λ-dimensional search can then be calculated using the formula

$$C(\Lambda) = \sum_{k=1}^{\Lambda} p(k) f_p(k) \qquad (26)$$

yielding

$$C(\Lambda) \leq \sum_{k=1}^{\Lambda} f_p(k) \sum_{q=0}^{\infty} \varphi\left(\frac{\frac{\phi_k^2}{4}}{2(\sigma^2+q)}, \frac{k}{2}\right) \cdot r_k(q) \qquad (27)$$

where $f_p(k) = 2k + 11$ denotes the number of numerical operations per visited node [17] in the k-th search layer.

While the inner summation in (27), has infinite terms, it can be seen that the terms $\varphi(\phi_k^2/4/2(\sigma^2+q), k/2) \cdot r_k(q)$ tends to zero for large q. We therefore approximate these expressions using a sum limit of $q_{\max} = 100$ when numerically calculating the complexity in terms of numbers of operations.

C. Complexity of Each of the SVP Sub-Schemes

We have up to now established the complexity associated with a generic Λ-dimensional sphere search. For each of the proposed selection techniques however, a number of sphere searches of variable dimensionality is required. We therefore use the above analysis combined with the algorithmic operations shown above to derive the complexity of each of the SVP sub-techniques. These complexities as a function of $C(\Lambda)$ are summarized in Table IV. As the rest of the transmit and receive processing is identical for conventional VP and all SVP

[1]Note that in the results section we use a search lattice with finite limits. For the case of a finite lattice, the subset of lattice points inside the hypersphere is dependent on the limits of the lattice and no generic closed form expression for the number of lattice points exists [17]. We therefore look at the generic case of an infinite lattice to attain a generic complexity expression at this point.

TABLE IV
COMPLEXITY FOR VP AND THE PROPOSED SVP SCHEMES

VP	$C(M) = \sum_{k=1}^{M} p(k) f_p(k)$
SVP-RS	$C_{RS} = \sum_{k=1}^{L} p(k) f_p(k)$
SVP-OS	$C_{OS} = \frac{M!}{(M-L)!L!} \left(1 + \sum_{k=1}^{L} p(k) f_p(k)\right)$
SVP-DS	$C_{DS} = (1 + p(1) f_p(1))\, M + \sum_{k=1}^{L} p(k) f_p(k)$
SVP-SS	$C_{SS} = \sum_{k=1}^{L} (M-k+1) \left(1 + \sum_{n=1}^{k} p(n) f_p(n)\right)$

schemes, in the analysis below we focus on the complexity associated with the sphere search.

1) SVP-RS: The symbols are chosen randomly and then an L-dimensional search is carried out. This clearly entails the least complexity of the proposed schemes given by

$$C_{RS} = C(L) = \sum_{k=1}^{L} p(k) f_p(k) \tag{28}$$

2) SVP-OS: For the optimal selection scheme, all possible $\binom{M}{L}$ combinations of L symbols are evaluated, each yielding an L-dimensional search, and the one with minimum norm is selected. The associated complexity is therefore given as

$$\begin{aligned} C_{OS} &= C(L)\binom{M}{L} + \binom{M}{L} \\ &= \frac{M!}{(M-L)!L!} \left(1 + \sum_{k=1}^{L} p(k) f_p(k)\right) \end{aligned} \tag{29}$$

Which is the sum of the numerical operations involved in the sphere searches plus the operations required to find the minimum amongst the $\binom{M}{L}$ norms.

3) SVP-DS: The decoupled selection involves M sphere searches of dimension 1 each to evaluate the minimum norm achieved with each symbol individually, and selecting the L symbols with lowest minimum norms. The SVP-DS subsequently carries out an L-dimensional search with the selected group of symbols. The complexity for this case is given as

$$\begin{aligned} C_{DS} &= C(1)M + M + C(L) \\ &= (1 + p(1) f_p(1))\, M + \sum_{k=1}^{L} p(k) f_p(k) \end{aligned} \tag{30}$$

4) SVP-SS: Finally the sequential selection initially picks the user that yields the minimum norm by individual perturbation, and at the k-th stage adds the user that minimizes the norm by joint perturbation with the previously selected users, until L users are selected. This involves $M-k+1$ searches of dimension k at the k-th stage, for which case the total complexity for this scheme is given as

$$\begin{aligned} C_{SS} &= \sum_{k=1}^{L} C(k)(M-k+1) + (M-k+1) \\ &= \sum_{k=1}^{L} (M-k+1) \left(1 + \sum_{n=1}^{k} p(n) f_p(n)\right) \end{aligned} \tag{31}$$

V. ENERGY EFFICIENCY

As the ultimate metric for evaluating the performance-complexity tradeoff and the overall usefulness of each of the proposed techniques and towards an energy efficient communication system, we look at the transmit energy efficiency of SVP compared to VP, and its dependence on the number of perturbed users L and the user selection method. Following the modeling of [20], [30], [31] we define the transmit energy efficiency of the communication link as the bit rate per total transmit power consumed i.e. ratio of the sum rate achieved over the consumed power at the transmitter

$$\mathcal{E} = \frac{R}{P_{PA} + N \cdot P_0 + p_c \cdot \tilde{C}} \tag{32}$$

where $P_{PA} = (\xi/\eta)P$ in Watts is the power consumed at the power amplifier to produce the total transmit signal power P, with η being the power amplifier efficiency and ξ being the modulation-dependent peak to average power ratio (PAPR). $P_0 = P_{mix} + P_{filt} + P_{DAC}$ is the power related to the mixers and transmit filters and the digital-to-analog converter (DAC), assumed constant for the purposes of this work. We use practical values of these from [31] as $\eta = 0.35$ and $P_{mix} = 30.3$ mW, $P_{filt} = 2.5$ mW, $P_{DAC} = 1.6$ mW yielding $P_0 = 34.4$ mW. p_c in Watts/KOps is the power per 10^3 elementary operations (KOps) of the digital signal processor (DSP) and $\tilde{C}$ is the average numbers of operations discussed above for each symbol selection case. This term is used to introduce complexity as a factor the transmitter power consumption in the energy efficiency metric. Typical values of p_c include $p_c = 22.88$ mW/KOps for the Virtex-4 and $p_c = 5.76$ mW/KOps for the Virtex-5 FPGA family from Xilinx [32]. In $\tilde{C}$ we use the fact that the sphere search and related optimization dominates the signal processing complexity at the transmitter and therefore the additional processing such as the scaling and modulo operation entail negligible complexity. Finally, R represents the sum rate which we discuss in the next subsection.

The expression in (32) provides a metric that combines transmission rate, complexity and transmit signal power, all in a unified metric. By varying the number of perturbed users L, both the resulting complexity and transmission rates are influenced, as shown above. Therefore, this expression can be used for the design of the communication link to maximize the energy efficiency by optimizing L and choosing the appropriate symbol selection scheme. High values of $\mathcal{E}$ indicate that high sum rates are achievable for a given transmit power consumption, and thus denote a high energy efficiency. The proposed technique is clearly advantageous in low transmit power scenarios, such as the small cell transmission, where the computational complexity accounts for a significant part of the power consumption attributed to the signal processing at the transmitter. The following results, however, show that SVP provides an increased energy efficiency compared to VP in numerous scenarios with varied transmit powers P.

A. Sum Rate Performance

In [33] the sum rate performance of VP was studied analytically and rate lower bounds were derived for a VP system with uniformly distributed inputs is given as

$$R = M \log \frac{E_b}{N_0 \pi e E\{\beta\}} + 2M\Omega\left(\frac{E\{\beta\}}{2\frac{E_b}{N_0}}\right) \tag{33}$$

where E_b and N_0 represent the energy per bit and noise spectral density respectively, and

$$\Omega(x) = \frac{1}{2} + \int_{-\frac{1}{2}}^{\frac{1}{2}} \sum_{s=-\infty}^{\infty} \frac{1}{\sqrt{2\pi x}} e^{-\frac{|\xi - s|^2}{2x}} \left(\sum_{t=-\infty}^{\infty} e^{-\frac{|\xi - t|^2}{2x}} \right) d\xi \tag{34}$$

is a function that relates to the effect of the receive modulo operation [6]. We note that while L users have their symbols perturbed as per the proposed scheme, it is M symbols that are transmitted per channel use, which justifies the use of M as the pre-log factor. For the high SNR region it was shown in [33] that

$$\lim_{\frac{E_b}{N_0} \to \infty} \Omega\left(\frac{E\{\beta\}}{2\frac{E_b}{N_0}}\right) = 0 \tag{35}$$

for which case a lower bound can be derived as

$$R \geq R_b = M \log \frac{E_b}{N_0 \pi e E\{\beta\}} \tag{36}$$

In the following, we use (36) in (32) to evaluate the energy efficiency of the conventional and proposed schemes.

VI. Numerical Results

This section presents numerical results based on Monte Carlo simulations of the proposed SVP techniques and conventional VP ($L = N$) for the frequency flat Rayleigh fading statistically uncorrelated MIMO channel whose impulse response is assumed perfectly known at the transmitter. Without loss of generality for the error rate results it is assumed that $P = 1$, while in the following energy efficiency results we use various values of P according to existing standards. A system employing 4-QAM modulation is explored for the case with $N = M$ while it is clear that the benefits of the proposed technique extend to non-symmetric MIMO channels and higher order modulation. We focus on the performance and complexity comparisons and tradeoff between VP and SVP. As explained above and following the methodology in the literature, here the complexity evaluation focuses only on the complexity of the tree-search stage, ignoring pre- and post-processing. To focus on the proposed concept, we compare the proposed SVP solely to conventional VP, while it is clear the benefits of the selective perturbation concept extend to modified VP designs existing in the literature. In the following we use the notation $\rho = 10\log_{10}(E_b/N_0)$ for convenience.

Fig. 4 shows the symbol error rate (SER) performance with the transmit SNR (ρ) for CI, VP and the proposed SVP schemes, for $L = 2$ perturbed users with $N = M = 10$. It can

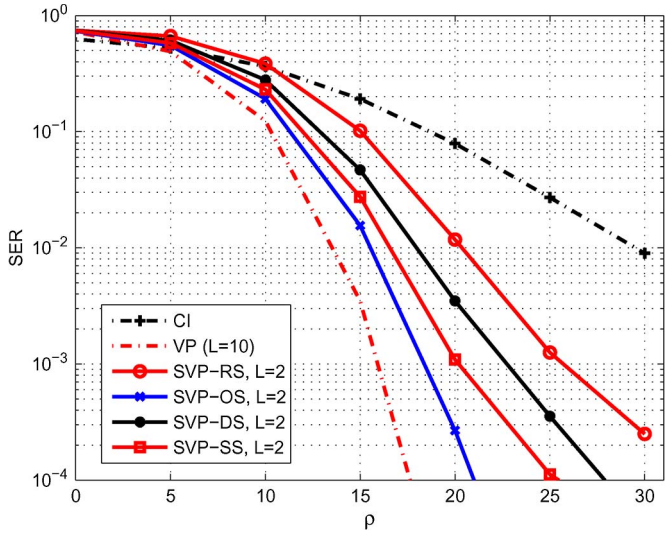

Fig. 4. SER vs. SNR for CI, VP, SVP, $N = M = 10$, $L = 2$, 4-QAM.

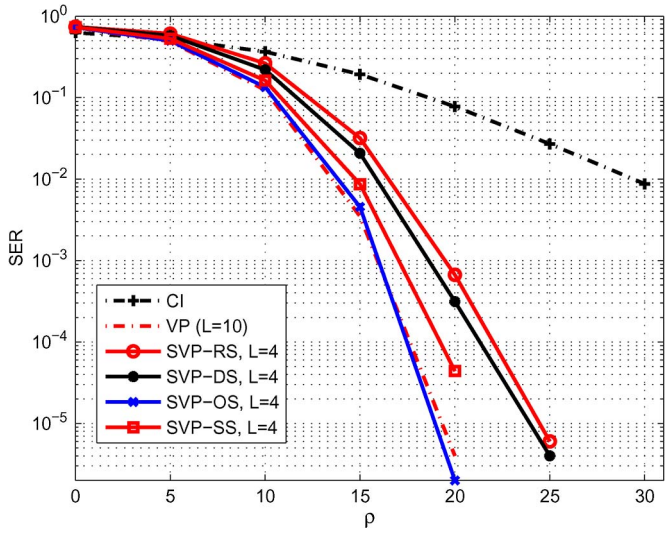

Fig. 5. SER vs. SNR for CI, VP, SVP, $N = M = 10$, $L = 4$, 4-QAM.

be seen that all the proposed schemes provide a performance between that of conventional VP and CI, with SVP-RS offering the worst performance due to the random user selection. Indeed, SVP-OS shows a significant improvement over SVP-RS with a 7 dB SNR gain and with only $L = 2$ perturbed users closely approaches the diversity and performance of full VP with $L = 10$. This however comes at the cost of increased complexity w.r.t. SVP-RS as detailed in the following. It should be noted however that the two other schemes namely SVP-DS and SVP-SS already offer 2.5 dB and 5 dB gains compared to SVP-RS with little added complexity.

This is further pronounced in Fig. 5 where the same comparison is shown for the case of $L = 4$. In this case SVP-OS achieves the performance of full VP with only $L = 4$. However, it is shown in the following that the complexity of SVP-OS in this case is comparable to the one for VP due to the large number of candidate transmit symbol groups. Nevertheless, it should be observed that the rest of the SVP schemes perform very close to VP at much reduced complexity (see Fig. 7). The

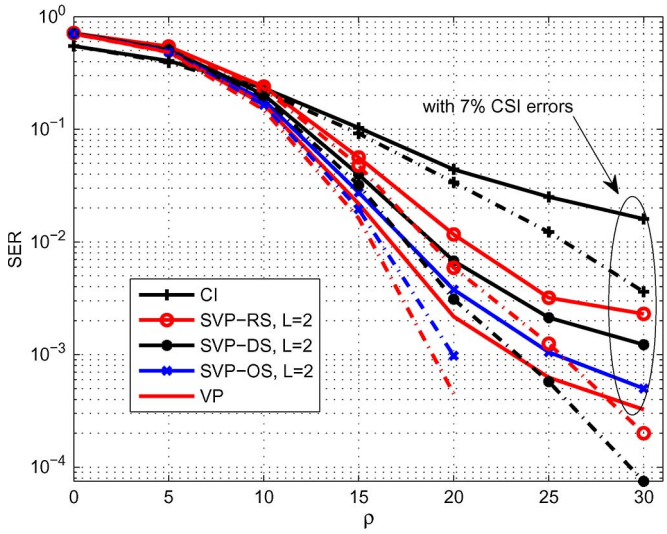

Fig. 6. SER vs. SNR for CI, VP, SVP, $N = M = 4$, $L = 2$, 4-QAM.

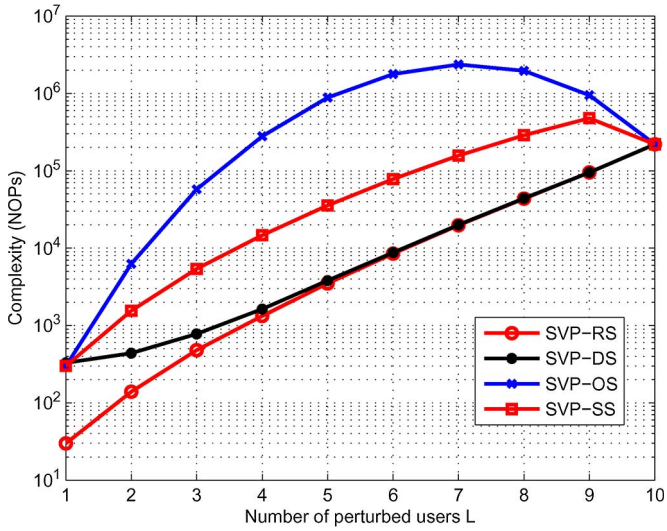

Fig. 7. Complexity for SVP with increasing L, $N = M = 10$, 4-QAM.

same trend can be seen in Fig. 6 where the SER is shown for the case of $N = M = 4$ with $L = 2$ perturbed users. In this figure we also show the performance of the techniques in the presence of 7% CSI errors at the transmitter and it can be seen that the performance of both VP and proposed SVP schemes deteriorates with the same trend. We note that for the cases with imperfect CSI at the transmitter, CSI-robust VP solutions such as the ones in [33]–[35] can be applied on top of the proposed SVP scheme to improve performance.

Fig. 7 shows the complexity in numbers of operations (NOPs) with increasing numbers of perturbed users L for the 10×10 MISO system ($N = M = 10$). We have calculated the average complexity per search empirically, which we then use in the complexity expressions in Table II to obtain the graphs shown. Clearly, the lowest complexity is offered by SVP-RS, closely followed by SVP-DS. It should be noted that the complexity of full VP corresponds to the case $L = M$. It is also observed that SVP-OS quickly becomes impractical from $L = 5$ onwards since it imposes complexity higher than con-

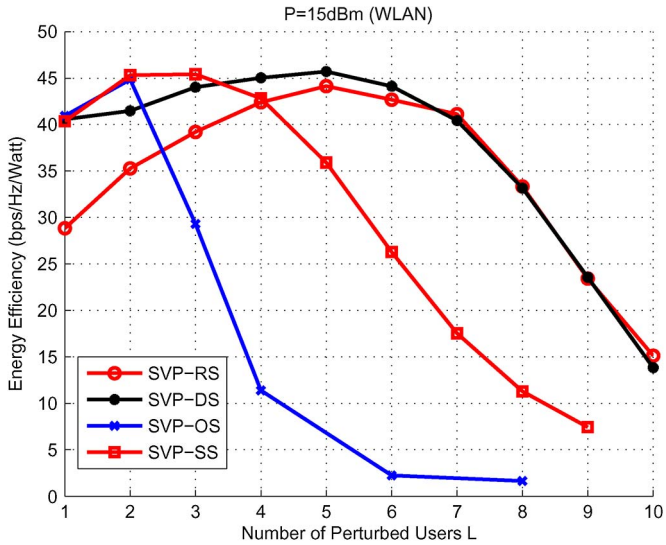

Fig. 8. Energy efficiency for SVP with increasing L, $N = M = 10$, $P = 15$ dBm (32 mW), $\rho = 20$ dB, 4-QAM.

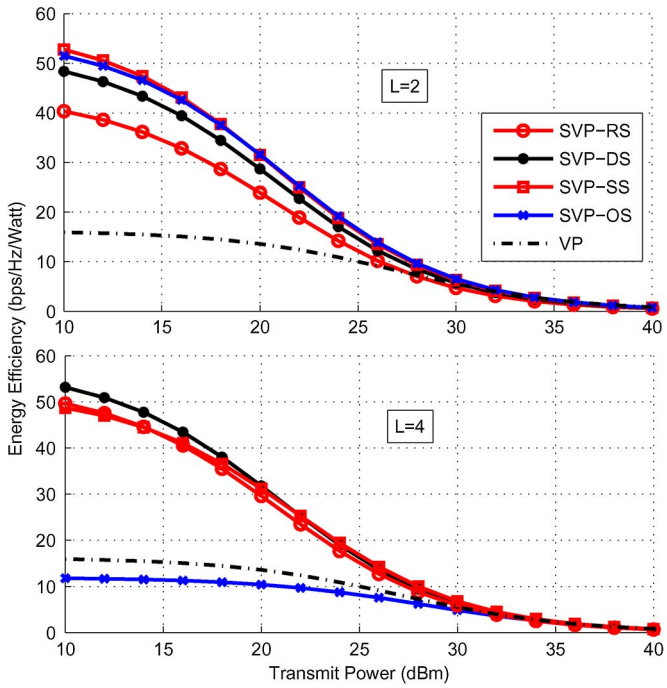

Fig. 9. Energy efficiency for SVP with increasing P for $L = 2$ and $L = 4$, $N = M = 10$, $\rho = 20$ dB, 4-QAM.

ventional VP. This is because, despite the fact that it involves sphere searches of reduced dimension, these need to be performed an amount of times $\binom{M}{L}$ which becomes excessive for larger L, leading to a high number of candidate perturbed symbol groups. The lower-complexity alternatives however still offer computational gains w.r.t. VP.

The performance complexity tradeoff for SVP is examined directly in Figs. 8–11 by means of the energy efficiency as defined in (32), for the 10×10 system with a fixed transmit SNR of $\rho = 20$ dB. Firstly for the transmit power of $P = 32$ mW (15 dBm) which corresponds to the power budget of a WLAN base station, it is clear that there is room for improving the efficiency of conventional VP which corresponds

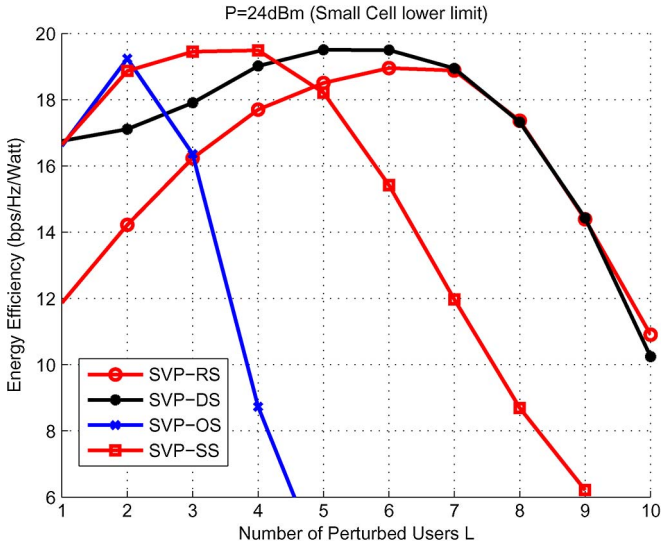

Fig. 10. Energy efficiency for SVP with increasing L, $N = M = 10$, $P = 24$ dBm (250 mW), $\rho = 20$ dB, 4-QAM.

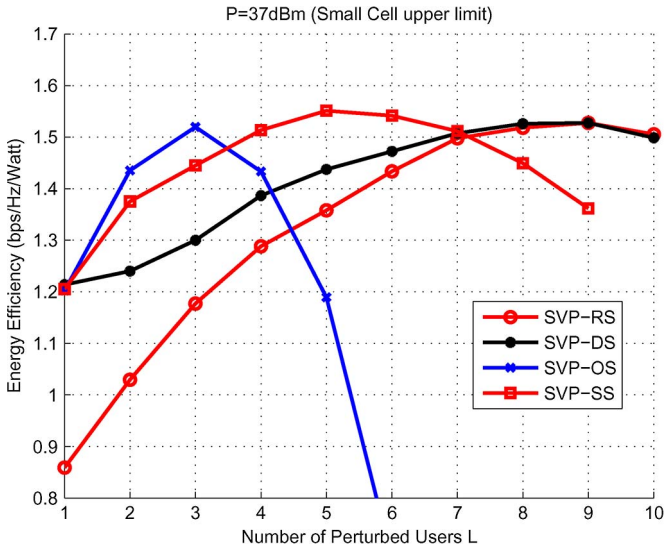

Fig. 11. Energy efficiency for SVP with increasing L, $N = M = 10$, $P = 37$ dBm (5 W), $\rho = 20$ dB, 4-QAM.

to the points with $L = 10$. It can be seen that for the different SVP schemes, different optimal values are found for L where the energy efficiency is maximized. The most power efficient options for this scenario are SVP-OS with $L = 2$ and SVP-DS with $L = 5$, both offering a power efficiency improvement compared to VP of more than 300%.

Fig. 9 illustrates the resulting energy efficiency of VP and the SVP schemes for increasing transmit powers from $P = 10$ dBm (10 mW) up to $P = 40$ dBm (10 W), which corresponds to the LTE base station power region, for the cases of $L = 2$ and $L = 4$. It can be seen that the energy efficiency of all schemes is reduced with increasing transmit power according to the metric in (32) due to the increase of the power consumption of the power amplifier. Note however, that all SVP schemes offer significant benefits in the energy efficiency compared to VP for power budgets of up to 30 dBm, with the exception of SVP-OS for $L = 4$ due to its impractical complexity.

The same comparison as in Fig. 8 is shown in Figs. 10 and 11 for transmit power budgets of $P = 250$ mW (24 dBm) and $P = 5$ W (37 dBm) respectively, which correspond to the limits of the transmit power envisaged for the small-cell deployment [36]. It can be observed that with increasing P the maxima of energy efficiency move to higher values of L for all techniques since the power consumption due to the added complexity becomes less significant compared to the gains in sum rates. Still however, the energy efficiency is maximized with the various SVP schemes at values of $L < M$. It can therefore be concluded that the proposed scheme provides a more power efficient alternative to VP for the low power transmission of future small cell networks.

VII. Conclusion

An selective vector precoding scheme has been proposed, which partially perturbs the information symbols to improve the energy efficiency of VP. By applying the perturbation function to a subset of the transmit symbols, the proposed scheme saves significant computational complexity which otherwise increases exponentially with the number of users. To improve the resulting tradeoff between performance and complexity, a number of criteria have been proposed for the selection of the symbols to be perturbed, yielding significant performance gains. The results show that the proposed SVP schemes provide significant energy efficiency gains with respect to conventional VP, especially in the low-power transmission envisaged for the future generation of communication networks.

References

[1] *Evolved Universal Terrestrial Radio Access (E-UTRA); Physical Channels and Modulation*, 3GPP TS 36.211 V8.2.0 (2008-03), Release 8, 2008.
[2] M. Costa, "Writing on dirty paper," *IEEE Trans. Inf. Theory*, vol. IT-29, no. 3, pp. 439–441, May 1983.
[3] U. Erez, S. Shamai, and R. Zamir, "Capacity and lattice strategies for cancelling known interference," *IEEE Trans. Inf. Theory*, vol. 51, no. 11, pp. 3820–3833, Nov. 2005.
[4] B. Hassibi and H. Vikalo, "On the expected complexity of integer least squares problems," in *Proc. IEEE Int. Conf. Acoust., Speech, Signal Process.*, Orlando, FL, USA, May 2002, pp. 1497–1500.
[5] C. Windpassinger, R. Fischer, T. Vencel, and J. Huber, "Precoding in multiantenna and multiuser communications," *IEEE Trans. Wireless Commun.*, vol. 3, no. 4, pp. 1305–1316, Jul. 2004.
[6] C. Masouros, M. Sellathurai, and T. Rantarajah, "Interference optimization for transmit power reduction in Tomlinson-Harashima precoded MIMO downlinks," *IEEE Trans. Signal Process.*, vol. 60, no. 5, pp. 2470–2481, May 2012.
[7] A. Garcia and C. Masouros, "Power-efficient Tomlinson-Harashima precoding for the downlink of multi-user MISO systems," *IEEE Trans. Commun.*, vol. 62, no. 6, pp. 1884–1896, Jun. 2014.
[8] C. B. Peel, B. M. Hochwald, and A. L. Swindlehurst, "A vector-perturbation technique for near-capacity multiantenna multiuser communication—Part I: Channel inversion and regularization," *IEEE Trans. Commun.*, vol. 53, no. 1, pp. 195–202, Jan. 2005.
[9] C. Masouros and E. Alsusa, "Dynamic linear precoding for the exploitation of known interference in MIMO broadcast systems," *IEEE Trans. Wireless Commun.*, vol. 8, no. 3, pp. 1396–1404, Mar. 2009.
[10] C. Masouros, "Correlation rotation linear precoding for MIMO broadcast communications," *IEEE Trans. Signal Process.*, vol. 59, no. 1, pp. 252–262, Jan. 2011.
[11] Z. Ding and H. V. Poor, "A general framework of precoding design for multiple two-way relaying communications," *IEEE Trans. Signal Process.*, vol. 61, no. 6, pp. 1531–1535, Mar. 2013.

[12] C. Masouros and E. Alsusa, "Soft transmitter precoding for the downlink of DS/CDMA communication systems," *IEEE Trans. Veh. Technol.*, vol. 59, no. 1, pp. 203–215, Jan. 2010.
[13] C. Masouros, M. Sellathurai, and T. Ratnarajah, "Large-scale MIMO transmitters in fixed physical spaces: The effect of transmit correlation and mutual coupling," *IEEE Trans. Commun.*, vol. 61, no. 7, pp. 2794–2804, Jul. 2013.
[14] C. Masouros and E. Alsusa, "Two-stage transmitter precoding based on data-driven code hopping and partial zero forcing beamforming for MC-DCMA communications," *IEEE Trans. Wireless Commun.*, vol. 8, no. 7, pp. 3634–3645, Jul. 2009.
[15] C. B. Peel, B. M. Hochwald, and A. L. Swindlehurst, "A vector-perturbation technique for near-capacity multiantenna multiuser communication—Part II: Perturbation," *IEEE Trans. Commun.*, vol. 53, no. 3, pp. 537–544, Mar. 2005.
[16] J. Jalden and B. Ottersten, "On the complexity of sphere decoding in digital communications," *IEEE Trans. Signal Process.*, vol. 53, no. 4, pp. 1474–1484, Apr. 2005.
[17] B. Hassibi and H. Vikalo, "On the sphere-decoding algorithm I. Expected complexity," *IEEE Trans. Signal Process.*, vol. 53, no. 8, pp. 2806–2818, Aug. 2005.
[18] E. Agrell, T. Eriksson, A. Vardy, and K. Zeger, "Closest point search in lattices," *IEEE Trans. Inf. Theory*, vol. 48, no. 8, pp. 2201–2214, Aug. 2002.
[19] L. G. Barbero, T. Ratnarajah, and C. Cowan, "A comparison of complex lattice reduction algorithms for MIMO detection," in *Proc. IEEE ICASSP*, 2008, pp. 2705–2708.
[20] C. Masouros, M. Sellathurai, and T. Ratnarajah, "Computationally efficient vector perturbation precoding using thresholded optimization," *IEEE Trans. Commun.*, vol. 61, no. 5, pp. 1880–1890, May 2013.
[21] C. Masouros, M. Sellathurai, and T. Ratnarajah, "A low-complexity sequential encoder for threshold vector perturbation," *IEEE Commun. Lett.*, vol. 17, no. 12, pp. 2225–2228, Dec. 2013.
[22] B. Lee and B. Shim, "A vector perturbation with user selection for multiuser MIMO downlink," *IEEE Trans. Commun.*, vol. 60, no. 11, pp. 3322–3331, Nov. 2012.
[23] H. S. Han, S. H. Park, S. Lee, and I. Lee, "Modulo loss reduction for vector perturbation systems," *IEEE Trans. Commun.*, vol. 58, no. 12, pp. 3392–3396, Dec. 2010.
[24] S. H. Park, H. S. Han, S. Lee, and I. Lee, "A decoupling approach for low-complexity vector perturbation in multiuser downlink systems," *IEEE Trans. Wireless Commun.*, vol. 10, no. 6, pp. 1697–1701, Jun. 2011.
[25] U. P. Rico, E. Alsusa, and C. Masouros, "A fast least-squares solution-seeker algorithm for vector-perturbation," in *Proc. IEEE GLOBECOM*, Nov. 2008, pp. 1–5.
[26] R. Chen, C. Li, J. Li, and Y. Zhang, "Low complexity user grouping vector perturbation," *IEEE Wireless Commun. Lett.*, vol. 1, no. 3, pp. 189–112, Jun. 2012.
[27] H. Song, S. Choi, and D. Hong, "Line encoding for multiuser MIMO downlink," *IEEE Trans. Veh. Technol.*, vol. 60, no. 2, pp. 734–739, Feb. 2011.
[28] M. Sandell, H. Vetter, and F. Tosato, "Joint linear and nonlinear precoding in MIMO systems," *IEEE Commun. Lett.*, vol. 15, no. 12, pp. 1265–1267, Dec. 2011.
[29] C. P. Schnorr and M. Euchner, "Lattice basis reduction: Improved practical algorithms and solving subset sum problems," *Math. Programm.*, vol. 66, no. 1–3, pp. 181–191, Aug. 1994.
[30] X. Cong, G. Y. Li, Z. Shunqing, Y. Chen, and S. Xu, "Energy- and spectral-efficiency tradeoff in downlink OFDMA networks," *IEEE Trans. Wireless Commun.*, vol. 10, no. 11, pp. 3874–3886, Nov. 2011.
[31] S. Cui, A. J. Goldsmith, and A. Bahai, "Energy-constrained modulation optimization," *IEEE Trans. Wireless Commun.*, vol. 4, no. 5, pp. 2349–2360, Sep. 2005.
[32] D. Curd, Power Consumption in 65 nm FPGAs, Xilinx, White Paper, Feb. 2007.
[33] D. J. Ryan, I. B. Collings, I. V. L. Clarkson, and R. W. Heath, "Performance of vector perturbation multiuser MIMO systems with limited feedback," *IEEE Trans. Commun.*, vol. 57, no. 9, pp. 2633–2644, Sep. 2009.
[34] J. Maurer, J. Jaldén, D. Seethaler, and G. Matz, "Vector perturbation precoding revisited," *IEEE Trans. Signal Process.*, vol. 59, no. 1, pp. 315–328, Jan. 2011.
[35] C. Masouros, M. Sellathurai, and T. Ratnarajah, "Vector perturbation based on symbol scaling for limited feedback MISO downlinks," *IEEE Trans. Signal Process.*, vol. 62, no. 3, pp. 562–571, Feb. 2014.
[36] Small Cell Forum Ltd., W-CDM Open Access Small Cells: Architecture, Requirements and Dependencies, White Paper, May 2012.

Christos Masouros (M'06–SM'14) received the Diploma in electrical and computer engineering from the University of Patras, Patras, Greece, in 2004 and the M.Sc. degree by research and the Ph.D. degree in electrical and electronic engineering from the University of Manchester, Manchester, U.K., in 2006 and 2009, respectively.

He is currently a Lecturer with the Department of Electrical and Electronic Engineering, University College London, London, U.K. He previously held a Research Associate position at the University of Manchester and a Research Fellow position at the Queen's University Belfast, Belfast, U.K. He holds a Royal Academy of Engineering Research Fellowship from 2011–2016. His research interests lie in the field of wireless communications and signal processing, with particular focus on green communications, large-scale antenna systems, cognitive radio, interference mitigation techniques for MIMO, and multicarrier communications.

Mathini Sellathurai received the Technical Licentiate degree from the Royal Institute of Technology, Stockholm, Sweden, in 1997 and the Ph.D. degree from McMaster University, Hamilton, ON, Canada, in 2001. She is currently a Reader with Heriot-Watt University, Edinburgh, U.K. Her current research interests include adaptive and statistical signal processing, space–time and MIMO communications theory, network coding, information theory, and cognitive radio. She was the recipient of the Natural Sciences and Engineering Research Council of Canada's doctoral award for the Ph.D. dissertation and a corecipient of the IEEE Communication Society 2005 Fred W. Ellersick Best Paper Award. She is currently serving as an Associate Editor for the IEEE TRANSACTIONS ON SIGNAL PROCESSING.

Tharmalingam Ratnarajah (A'96–M'05–SM'05) is currently with the Institute for Digital Communications, The University of Edinburgh, Edinburgh, U.K., as a Reader in signal processing and communications. Since 1993, he has held various positions with Queen's University Belfast, Belfast, U.K.; University of Ottawa, Ottawa, ON, Canada; Nortel Networks, Ottawa, ON, Canada; McMaster University, Hamilton, ON, Canada; and Imperial College London, London, U.K. His research interests include random matrices theory, information theoretic aspects of MIMO channels and ad hoc networks, wireless communications, signal processing for communication, statistical and array signal processing, biomedical signal processing, and quantum information theory. He has published over 225 publications in these areas and holds four U.S. patents. He is currently the coordinator of the FP7 projects HARP (3.2 M€) in the area of highly distributed MIMO and ADEL (3.7 M€) in the area of dynamic spectrum access. Previously, he was the coordinator of the FP7 Future and Emerging Technologies project CROWN (2.3 M€) in the area of cognitive radio networks and HIATUS (2.7 M€) in the area of interference alignment. He is a member of the American Mathematical Society and Information Theory Society and a Fellow of Higher Education Academy (FHEA), U.K.